HHS Public Access

Author manuscript

Oncogene. Author manuscript; available in PMC 2015 July 22.

Published in final edited form as:

Oncogene. 2015 January 22; 34(4): 496–505. doi:10.1038/onc.2013.567.

KSHV vCyclin Counters the Senescence/G1 Arrest Response Triggered by NF-κB Hyper-activation

Huijun Zhi, **Muhammad Atif Zahoor**, **Abigail M. Druck Shudofsky**, and **Chou-Zen Giam***

Department of Microbiology and Immunology, Uniformed Services University of the Health Sciences, 4301 Jones Bridge Rd., Bethesda, MD 20814

Abstract

Many oncogenic viruses activate NF-κB as a part of their replicative cycles. We have shown recently that persistent and potentially oncogenic activation of NF-κB by the human T-lymphotropic virus 1 (HTLV-1) oncoprotein Tax immediately triggers a host senescence response mediated by cyclin-dependent kinase inhibitors: $p21^{CIP1/WAF1}$ (p21) and $p27^{Kip1}$ (p27) Here we demonstrate that RelA/NF-κB activation by Kaposi sarcoma herpesvirus (KSHV) latency protein vFLIP also leads to p21/p27 up-regulation and G1 cell cycle arrest. Remarkably, KSHV vCyclin, another latency protein co-expressed with vFLIP from a bicistronic latency-specific mRNA, was found to prevent the senescence and G1 arrest induced by HTLV-1 Tax and vFLIP respectively. This is due to the known ability of vCyclin/CDK6 complex to resist p21 and p27 inhibition and cause p27 degradation[23]. In KSHV-transformed BCBL-1 cells, sustained vFLIP expression with shRNA-mediated vCyclin depletion resulted in G1 arrest. The functional interdependence of vFLIP and vCyclin explains why they are co-translated from the same viral mRNA. Importantly, deregulation of the G1 cyclin-dependent kinase can facilitate chronic IKK/NF-κB activation.

Keywords

NF-κB hyper-activation; senescence; G1 cyclin-dependent kinase; CDK inhibitors; Kaposi's sarcoma herpesvirus; human T-lymphotropic virus type 1

Introduction

Kaposi's sarcoma (KS)-associated herpesvirus (KSHV), also known as human herpesvirus 8 (HHV-8), is a human γ-herpesvirus that causes Kaposi's sarcoma and two

*To whom correspondence should be addressed. Tel: 301-295-9624; Fax: 301-295-1545; chou-zen.giam@usuhs.edu.

Accession numbers

The GENBANK accession numbers or ID numbers for genes encoding the proteins described in this article are: KSHV *vCyclin*: U93872; *vFLIP*: U90534; HTLV-1 Tax: AB038239; p21: NM_000389; p27: NM_004064; Cyclin B1: NM_031966; I-κBα: NM_020529; p100/p52: NM_002502; p105/p50: NM_003998; RelA: NM_021975; RelB: NM_006509; and c-Rel: NM_002908.

Author contributions:

H. Z. and C-Z. G designed the experiments and wrote the manuscript. H. Z., M. A. Z., and A.M.D.S. performed experiments and data analyses.

Conflict of Interest:

The authors declare no competing financial interests related to the work described.

lymphoproliferative diseases known as body cavity-based B cell lymphoma or primary effusion lymphoma (PEL) and multi-centric Castleman's disease[1]. Like other herpesviruses, KSHV employs two distinct genetic programs, lytic replication and latency, for its propagation and persistence in infected host. During lytic replication, most viral genes are expressed in a temporally regulated manner. Viral DNA is replicated to high levels, with production of viral particles and eventual death of host cells. In latency, by contrast, only a handful of viral genes are expressed, and the viral genome is maintained in an episomal state at low levels. Host cells are stimulated to proliferate by proteins encoded by the latency genes, thus expanding the reservoir of latently infected cells. As KSHV latency gene products actively promote cell proliferation and survival, they constitute the thrust of KSHV carcinogenesis.

At least six viral proteins are expressed in cells latently infected by KSHV. Three of them, LANA (latency associated nuclear antigen, ORF73), vCyclin (ORF72), and vFLIP (ORF71) are encoded by one transcriptional unit through differential splicing[2,3]. The major unspliced 5.7 kb transcript directs the synthesis of LANA. A 1.7 kb spliced bicistronic mRNA contains vCyclin and vFLIP coding sequences in the 5' and 3' regions respectively[4]. Another latency gene locus directs the synthesis of a 1.4 kb mRNA transcript that encodes three proteins known as kaposin A, B, and C via differential initiation of translation (see[3] for review). LANA is responsible for the maintenance of the KSHV episome in latently infected cells and for the stabilization of β-catenin[5,6] and c-Myc[7], while vCyclin and vFLIP promote cell cycle progression and NF-κB activation respectively (reviewed in[3,8]). Kaposin A is a small hydrophobic cell surface protein that interacts with cytohesin-1, a guanine nucleotide exchange factor that regulates cell adhesion. Kaspoin B activates MK2, a kinase involved in regulating the stability of a specific group of mRNAs that contain the AU-rich elements (AREs) including those encoding myc, fos, VEGF, TNF, and GM-CSF. Finally, LANA2, a latency protein specifically expressed in B cells, has been shown to inactivate p53[9].

The potent activation of NF-κB by vFLIP is reminiscent of a similar activity of the human T-lymphotropic virus type I (HTLV-1) oncoprotein/trans-activator, Tax. Both KSHV vFLIP and HTLV-1 Tax directly interact with the regulatory subunit of I-κB kinases (IKKs), NF-κB essential modulator (NEMO)/IKKγ, and via a mechanism not fully understood, activate IKKα and IKKβ constitutively[10–13]. Chronic IKK activation, in turn, causes persistent degradation of all I-κBs, increased expression and proteolytic processing of NF-κB2 precursor, p100, and activation of both classical and alternative NF-κB pathways[14–16]. The oncogenic activity of Tax in cell culture and in transgenic mice has been shown previously to be driven by NF-κB[10,17–20]. Likewise, IKK/NF-κB activation by KSHV vFLIP has also been demonstrated to be crucial for the survival of pleural effusion lymphoma (PEL) cells[21].

We have found recently that persistent and potentially oncogenic stimulation of NF-κB by HTLV-1 Tax activates a defense mechanism/checkpoint response that commits cells into an irreversible state of cell cycle arrest known as senescence[22]. This checkpoint is triggered by hyper-activated p65/RelA and is mediated in part by two cyclin-dependent kinase inhibitors, $p21^{CIP1/WAF1}$ (referred to as p21) and $p27^{Kip1}$ (referred to as p27) in a p53- and pRb-independent manner[22]. Here we demonstrate that NF-κB activation by vFLIP causes p21-/p27-mediated cell cycle arrest in the G1 phase. Remarkably, KSHV vCyclin can prevent the

G1 cell cycle arrest/senescence induced by vFLIP and Tax respectively. KSHV vCyclin is known to interact preferentially with cellular cyclin-dependent kinase 6 (Cdk6); and the vCyclin/Cdk6 complex has been shown previously to resist $p16^{INK4a}$, p21, and p27 inhibition, and to target p27 for phosphorylation and degradation[23,24]. Indeed, we have found that in KSHV vCyclin-expressing HeLa cells, vFLIP- or Tax-induced up-regulation of p27 is significantly attenuated; and the surge in p21 is ineffective in causing G1 arrest/senescence. Based on these results, we speculate that up-regulation of D-type cyclins and loss of inhibitors of cyclin D-Cdks (such as $p16^{INK4a}$ or $p15^{INK4b}$) — genetic alterations frequently found in human cancers including adult T cell leukemia/lymphoma and multiple myeloma[25] — may functionally resemble KSHV vCyclin expression in causing p21/p27 sequestration and/or inactivation, thereby facilitating chronic NF-κB activation and leukemogenesis. Interestingly, while stable vCyclin expression was readily established in HeLa cells, it was not permissible in BJAB cells. This likely reflects cellular safeguard functional in BJAB, but defective in HeLa that protects against overly active cyclin-CDK6 activity.

Results

KSHV vFLIP induces p21-/p27-mediated G1 cell cycle arrest

We have shown previously that the potentially oncogenic hyper-activation of IKK/NF-κB by the HTLV-1 trans-activator/oncoprotein, Tax, triggers a cellular senescence response mediated by cyclin-dependent kinase inhibitor (CDKI) p27 and p21[22,26]. Since KSHV vFLIP is also a potent activator of IKK/NF-κB, the possibility that vFLIP may also induce senescence immediately arises. To answer this question, we subcloned the wild-type and the Flag-tagged vFLIP[27] coding sequences into a lentivirus vector, HR-CMV-SV-puro, to produce LV-vFLIP-puro and LV-vFLIP-Flag-puro, respectively. Lentivirus vectors for vFLIP were then generated and used to transduce the HeLa-G reporter cell line as previously described[26]. The HeLa-G cell line contains a Tax reporter cassette, 18×21-EGFP, composed of the enhanced green fluorescent protein (EGFP) gene under the transcriptional regulation of 18 copies of the Tax-responsive 21-bp enhancer element; and expresses abundant GFP upon Tax expression[28]. After LV-vFLIP-Puro, LV-Tax-Puro, or LV-Puro transduction for 2 days, HeLa-G cells were trypsinized and plated sparsely as single cells, and selected in puromycin-containing medium. As shown in Fig. 1A, cells stably transduced by the vFLIP vector became elongated and ceased proliferation soon after vFLIP expression as suggested by the low density of LV-vFLIP-transduced cells 6 and 8 days post-transduction (Fig. 1A LV-vFLIP). As previously reported, LV-Tax-transduced (GFP-positive) HeLa-G cells underwent 1–2 rounds of division and ceased proliferation (Fig. 1A LV-Tax). In contrast, under the same condition, cells transduced by the control LV-puro vector grew and became confluent (Fig. 1A LV-puro). Compared to the control, cells expressing vFLIP had drastically reduced levels of I-κBα and heightened expression and processing of p100 (Fig. 1B lane 1 versus lanes 3 and 4, see figure legend for quantitation), consistent with the ability of vFLIP to potently activate both the classical and the alternative NF-κB pathways[13,21,29,30]. As expected, in vFLIP (or vFLIP-Flag)-expressing cells, the levels of p21 and p27 were drastically elevated (approximately 6–9 fold, see Fig. 1 legend for quantitation) with a concomitant reduction in cyclin B1 levels (Fig. 1B lane 1 [100%] versus

lanes 3 [19%] and 4 [8%]). This is in agreement with a cessation of cell cycle activities and similar to what was previously seen in Tax-expressing cells (Fig. 1B lane 2 [18%]). Indeed, flow cytometry of LV-vFLIP- versus LV-puro-transduced HeLa-G cells showed a substantial increase in G1 (Fig. 1C, 75.9% versus 50.6%) and a corresponding decrease in S and G2/M population after vFLIP expression (Fig. 1C). Likewise, growth curves of LV-puro versus LV-vFLIP-transduced cells indicated a cessation of cell proliferation after vFLIP expression (supplemental Fig. S1). In addition to their elongated morphology, vFLIP-expressing cells were found to be larger in size as reflected by a high degree of forward scatter in flow cytometry analysis (Fig. 1D). Even though vFLIP cells were elongated in shape, their nuclei appeared largely normal. This contrasts with Tax cells, which are often flattened, enlarged in a relatively isotropic manner, and have overt nuclear abnormalities such as bi-nucleation or micronuclei formation caused by a bypass of mitosis or a defect in mitosis prior to the onset of senescence arrest[26,31]. Importantly, more than 75% of Tax-transduced cells stained positive for senescence-associated β-galactosidase while less than 10% of vFLIP-transduced cells did so (Fig. 1E), suggesting that vFLIP causes primarily G1 cell cycle arrest with only a limited extent of senescence. We also examined Tax- and vFLIP-expressing HeLa-G cells for another senescence marker, the senescence associated heterochromatin foci (SAHF), but were unable to detect them (see supplemental Fig. S2). As mentioned above, Tax-, but not vFLIP-expressing cells showed frequent mitotic abnormalities (marked with arrows in Fig. S2 column 1 middle panel). These nuclear/mitotic abnormalities unique to Tax-expressing cells may underlie the senescence versus G1 arrest caused by Tax and vFLIP respectively.

KSHV vFLIP-induced G1 arrest is due to NF-κB hyper-activation

To determine if vFLIP-induced G1 arrest is NF-κB driven, we transduced LV-vFLIP-puro into HeLa-G and a HeLa-G-derived cell line, ΔN-I-κBαN4, whose NF-κB activity is blocked by the stable expression of ΔN-I-κBα, a degradation-resistant form of I-κBα lacking the NH_2-terminal 36 amino acid residues that constitute the motif for IKK phosphorylation and proteasome-mediated degradation[22]. Again, after LV-vFLIP-puro transduction for 48 hours, cells were selected in media containing 1 μg/ml puromycin, and then photographed at day 2 and day 5 after selection (Fig. 2A). As expected, the G1 arrest caused by vFLIP was effectively prevented in ΔN-I-κBαN4 cells (Fig. 2A, Day 5, compare left and right panels). Indeed, in ΔN-I-κBαN4 cells, even though vFLIP continued to induce the degradation of endogenous I-κBα, the NF-κB-dependent up-regulation of p100 by vFLIP was effectively abrogated by ΔN-I-κBα (Fig. 2B compare lanes 2 and 4). No down-regulation of cyclin B1 and up-regulation of p21 and p27 were detected in vFLIP-expressing ΔN-I-κBαN4 cells, in sharp contrast to the HeLa-G control (Fig. 2B compare lanes 1 and 2 versus 3 and 4).

We have previously derived HeLa-G cell lines that have been rendered deficient in RelA, RelB and p100, and c-Rel respectively by the stable expression of their respective small hairpin RNAs (shRNAs) (Fig. 3A). These cell lines have been used to show that only chronically activate RelA is responsible for Tax-induced senescence[22]. To investigate if the same holds true for vFLIP-induced G1 arrest, the Flag-tagged vFLIP (vFLIP-Flag) gene was transduced into control, RelA, dual RelB/p100, and c-Rel knockdown (KD) HeLa-G cell

lines via a lentivirus vector. Following LV-neo or LV-vFLIP-Flag-neo transduction, G418 selection was performed to select for stably transduced cells (see **Materials and Methods**). Cell lysates were then prepared from the parental HeLa-G control and each pool of KD cell lines for immunoblotting to detect vFLIP (via Flag epitope tag), markers of IKK/NF-κB activation (degradation of I-κBα and up-regulation of p100/p52), and indicators of cell cycle arrest (increase in p21 and p27). As shown in Fig. 3A, vFLIP activated both the classical and the alternative NF-κB pathways in control cells (lane 1 versus 2, lane 5 versus 6, and lane 9 versus 10). In RelA KD cells, vFLIP caused I-κBα degradation, but did not induce p100 expression, which depends on p50/RelA NF-κB (Fig. 3A lane 2 versus 4). This is as might be expected since RelA KD impaired NF-κB transcriptional activity, but had no effect on IKK activation by vFLIP. Importantly, and as previously reported for Tax[22], RelA KD prevented vFLIP-mediated up-regulation of p21 and p27 and allowed vFLIP-expressing cells to proliferate (Fig. 3B, 2nd column from left). In cells with dual p100/RelB (Fig. 3A center panel) or c-Rel knockdown (Fig. 3A right panel) as well as in control cells, vFLIP continued to down-regulate I-κBα and activate NF-κB (Fig. 3A lane 6 versus 8, and 10 versus 12). As expected, it increased p27 level in cells with the dual p100/RelB or the c-Rel knockdown (Fig. 3A lane 6 versus 8, and 10 versus 12). VFLIP did not significantly up-regulate p21 in p100/RelB knockdown cells, but did so in c-Rel knockdown, similar as previously observed for Tax[22]. The up-regulation of p21 and p27 in HeLa-G, p100/RelB knockdown, and c-Rel knockdown correlated with a cessation of cell division as indicated by the appearance of elongated cells that divided far less than their LV-Neo-transduced counterparts (Fig. 3B 1st, 3rd, and 4th columns from left to right). Together with the results in Fig. 2, these data support the thesis that vFLIP causes arrest at the G1 phase of the cell cycle. Like Tax-induced senescence, vFLIP-induced G1 arrest is driven by chronically activated RelA NF-κB and mediated by p21 and p27.

KSHV vCyclin prevents G1 arrest and mitigates cellular senescence induced by vFLIP and Tax respectively

KSHV vFLIP is co-expressed with another KSHV latency protein, vCyclin, in a bicistronic mRNA where vCyclin coding sequence reside in the 5’ end, followed by an internal ribosomal entry site that overlaps with the vCyclin coding sequence, and with the vFLIP coding region residing in the 3’ end[4,32,33]. The genetic link and co-expression of vFLIP and vCyclin suggest a close functional association. Indeed, it has been reported previously that vCyclin can induce senescence in primary foreskin fibroblasts; and vFLIP was found to prevent vCyclin-induced senescence through an interaction with ATG3[34] that blocks autophagy induction[34,35]. Notably, KSHV vCyclin has been shown to interact with cellular G1 cyclin-dependent kinase 6 (Cdk6) and activates its G1 and G1/S Cdk activities[23,24]. Upon association with KSHV vCyclin, Cdk6 phosphorylates p27, and targets it for degradation[23,24]. Further, the kinase activity of the vCyclin/Cdk6 complex is not inhibited by $p16^{INK4a}$, p21, and p27 CDK inhibitors[23]. Because p27 and p21 are the principal drivers of G1 arrest/senescence triggered by vFLIP and Tax, the said biological properties of vCyclin immediately suggest the interesting possibility that it may mitigate or prevent the G1 arrest/senescence response trigged by vFLIP and Tax respectively.

To test this hypothesis, we constructed a lentivirus vector, LV-2Flag-vCyc-puro, carrying the coding sequence of dual Flag epitope-tagged vCyclin, and used it to derive several vCyclin expressing HeLa-G cell lines. vCyclin has been shown previously to cause senescence in primary human endothelial cells due to induction of replicative stress and activation of the DNA damage response[36]. The vCyclin-induced senescence, however, is thought to depend on the tumor suppressor, p53. Since p53 is inactivated in HeLa cells by the E6 oncoprotein of HPV18, vCyclin-expressing HeLa cell lines were readily established after gene transduction and puromycin selection, and confirmed by immunoblotting (Fig. 4A and B). The analysis of one such cell line, vCyc-G2, is represented here. Flow cytometry indicated that the cell population in G1 phase of the cell cycle was significantly reduced in asynchronously grown vCyc-G2 cells, with a corresponding increase in the G2 phase (Fig. 4C). This is in accordance with the notion that vCyclin promotes cell cycle entry.

To assess the effect of vCyclin on preventing NF-κB-induced senescence or G1 arrest, we transduced sparsely plated HeLa-G and vCyc-G2 cells respectively with the Ad-Tax vector at an MOI of 1 and monitored the transduced cells over a course of 5 days. GFP-positive (Tax-expressing) HeLa-G cells ceased division shortly after Ad-Tax was introduced and appeared as singlet or doublet (Fig. 5A left panels), as previously reported[22,31]. By contrast, GFP-positive vCyc-G2 cells continued to grow and divide after Ad-Tax transduction (Fig. 5A right panels), indicating that the senescence response triggered by Tax was effectively blocked by vCyclin. Similarly, HeLa-G and vCyc-G2 cells were transduced with LV-vFLIP-Flag-neo, and then selected in G418 for 6 days. As expected, vCyclin effectively prevented the G1 arrest induced by vFLIP in control HeLa-G cells, thereby allowing vFLIP-expressing vCyc-G2 cells to grow and divide (compare Fig. 5B left and right panels).

We next examined the biochemical markers of G1 arrest and its ablation in HeLa-G cells versus vCyc-G2 cells. Each cell line was transduced with vFLIP or Tax lentivirus vector. As both lentiviral vectors contain the neomycin-resistance gene, transduced cells were subject to G418 selection for 4 days. Cells were harvested and their lysates analyzed by immunoblotting (Fig. 5C). As expected, expression of vFLIP and Tax in both HeLa-G and vCyc-G2 cells caused I-κBα degradation and dramatic up-regulation of p100 expression, indicating persistent IKK/NF-κB activation (Fig. 5C lanes 2 3, 5, and 6 versus lanes 1 and 4). Importantly, vFLIP only increased p21 and p27 levels modestly (2.2 and 1.5 fold respectively) and did not significantly down-regulate cyclin B1 in vCyc-G2 cells (88%), in dramatic contrast to the HeLa-G control (17% see Fig. 5C lane 3 versus 6). The expression of Tax in vCyc-G2 cells continued to up-regulate p21 and p27 (6.1 and 5.8 fold respectively), albeit to a lesser extent than in HeLa-G control (7.2 and 8.3 fold respectively, see Fig. 5C lane 5 versus 2). Further, the decrease in cyclin B1 level of HeLa-G cells caused by Tax (lane 2), while not fully restored by vCyclin to the control level, was not as severe (compare Fig. 5C lanes 2 versus 5, 29% versus 65% of control). This is consistent with the ability of vCyclin to allow Tax-expressing vCyc-G2 cells to continue to grow and divide (Fig. 5A). Finally, stable HeLa cell lines whose IKK/NF-κB pathway is chronically activated can be established by the sequential transfer of vCyclin and Tax genes (see supplemental Fig. S3A, vCyclin only [lane 2] versus vCyclin + Tax [lanes 3–5 for three independently isolated clones); vCyclin and vFLIP genes (Fig. S3C, vCyclin only [lane 2] versus vCyclin + vFLIP [lanes 3 and 4, two clones]; or in a single step by using bicistronic

v-Cyclin-Tax (Fig. S3A, lanes 6 and 7, two clones) and bicistronic vCyclin-vFLIP (Fig. S3D lanes 3–5, three clones) expression vectors depicted in Fig. S3B.

KSHV vFLIP causes G1 arrest in BCBL-1 upon KSHV vCyclin depletion

While vCyclin could be readily expressed in HeLa cells, its expression in other cultured cell lines including BJAB was not permissible. BJAB cells transduced with vFLIP and vCyclin either individually or in combination expressed the respective proteins early after antibiotic selection, but soon lost expression in successive cell passages (Fig. S4A). Consistent with the notion that chronic expression of vFLIP is disfavored, vFLIP up-regulated p21 and p27 expression in BJAB cells (Fig. S4B, lane 1 versus 3). While vCyclin down-regulated p27 in BJAB cells (Fig. S4B lane versus 2), it induced apoptosis (see[37,38] and unpublished data). Thus, cell cycle arrest and apoptosis, respectively, precluded vFLIP or vCyclin from being stably expressed in BJAB cells.

To confirm the synergism between vCyclin and vFLIP in human B cells, we stably transduced a KSHV-transformed cell lines BCBL-1 with LV-vFLIP-Flag-Neo followed by G418 selection. The expression of vCyclin in BCBL-1/FLIP-Flag cells was then knocked down using an shRNA targeted to vCyclin. We reason that because endogenous vCyclin and vFLIP in BCBL-1 cells are co-expressed from a bicistronic mRNA, the shRNA-mediated knockdown of vCyclin would cause the endogenous vFLIP to be down-regulated, but would have no effect on expression of the exogenously transduced vFLIP-Flag gene. This would allow the synergism of vFLIP and vCyclin to be assessed in a relevant cell type.

In accordance with the results in Fig. 1, BCBL-1 cells constitutively express vFLIP, which causes chronic IKK/NF-κB activation as reflected by I-κBα degradation (Fig. 6A compared BJAB and BCBL-1, lane 1 versus 2). Consistent with the induction of a cellular senescence/G1 arrest response by vFLIP, BCBL-1 cells express elevated levels of p21 and p27 compared to the KSHV-unrelated BJAB control (Fig. 6A lane 1 versus 2). Additional expression of Flag-tagged vFLIP in BCBL cells further induced a small increase in p21 and p27 levels (Fig. 6A lane 3 versus 2). This, in turn, moderately inhibited cell cycle entry of BCBL-1 as indicated by an increase of cell population in G1 and a decrease in S and G2/M phases in the vFLIP-Flag-transduced cells (Fig. 6B). Depletion of endogenous vCyclin and vFLIP by an shRNA targeted to vCyclin (Fig. 6C) caused the majority of BCBC-1/vFLIP-Flag cells to be arrested in G1 (Fig. 6D, approximately 65% G1 versus 84% G1, with versus without vCyclin) with elevated p21/p27 expression and much reduced cyclin B1 level compared to the control (Fig. 6C lane 2 versus 1). These results support the conclusion that vCyclin counters the G1 arrest/ senescence response triggered by vFLIP-driven NF-κB hyper-activation.

Discussion

We have shown previously that hyper-activation of NF-κB by Tax triggers a cellular senescence response driven in part by CDK inhibitors p21 and p27[22]. The present study of KSHV vFLIP extends that conclusion and provides another example of a viral activator of IKK/NF-κB causing p21/p27 up-regulation and G1 cell cycle arrest in HeLa and human B cells. In contrast to Tax, which induces senescence within one cell cycle, vFLIP causes

primarily G1 arrest; and the extent of cellular senescence it induces is moderate (Fig. 1E, less than 10% for vFLIP versus greater than 75% for Tax). Although p21 and p27 play key roles in the cell cycle arrest caused by both Tax and vFLIP, a significant fraction of Tax-, but not vFLIP-expressing cells show mitotic aberrations as reflected by increased nuclear sizes, binucleation, and micronuclei formation (supplemental figure S2). The reason for these phenotypic differences between vFLIP and Tax is unclear, but may be related to the cellular factors utilized by each protein to activate IKK. Thus, while p21 and p27 up-regulation causes G1 arrest, it appears necessary but not sufficient for robust senescence induction. Importantly, an in-depth examination of KSHV vCyclin, a protein co-expressed with vFLIP in a bicistronic KSHV latency mRNA transcript, revealed that vCyclin effectively prevented or mitigated the G1 arrest/senescence response induced by vFLIP and Tax respectively. Indeed, when vCyclin expression is knocked down in KSHV-transformed BCBL-1 cells, continuing expression of vFLIP led to G1 arrest (Fig. 6). Thus, unlike HTLV-1, KSHV utilizes vCyclin to form a G1 vCyclin-CDK complex that resists p21 and p27 inhibition and targets p27 for degradation[8,23,24,39], thereby rendering vFLIP (and Tax)-driven chronic IKK/NF-κB activation permissible. The collaborative interaction between vCyclin and vFLIP is further highlighted by recent studies showing that vFLIP blocks vCyclin-induced senescence in primary foreskin fibroblasts[35]. This activity correlates with the ability of vFLIP to interact with ATG3 and prevent autophagy induction[34,35]. In aggregate, present results and published data support the notion that vCyclin and vFLIP act in concert to promote the proliferation (via Cdk6 activation) and survival (via NF-κB activation) of cells that are latently infected by KSHV. These results are summarized in Fig. 7.

VFLIP-expressing HeLa cells are phenotypically different from their Tax-expressing counterparts, which often progress through S and G_2, bypass mitosis, and then enter into senescence/irreversible G_1 arrest[26,31]. Because of mitotic/cytokinesis failure, the Tax-expressing senescent HeLa (and other adherent) cells become enlarged (with at least twice the normal cytoplasmic and DNA contents) and flattened with extensive nuclear abnormalities[31]. By contrast, vFLIP-expressing HeLa cells are elongated and their nuclei appear relatively normal (Fig. 1E). It has been known that KSHV-infected endothelial cells assume the shape of a spindle; and importantly, the spindle cell morphology was previously shown to be a result of IKK/NF-κB activation[27]. The underlying cause for the morphological differences between Tax- and vFLIP-expressing cells remains unclear.

While KSHV vCyclin can be stably expressed in HeLa cells, expression of vCyclin in primary cells causes DNA replicative stress and p53-dependent senescence[36,40]. The tumor suppressor, p53, in HeLa cells is targeted for degradation by the HPV-18 E6 protein. This loss of p53 likely contributed to the ease of stable vCyclin expression in HeLa cells. Surprisingly, in the BJAB human B cell line, vCyclin expression was still disfavored due to cellular apoptosis, which occurred despite a missense H193R mutation in the p53 gene of BJAB that renders p53 nonfunctional[37]. While this outcome precludes the possibility of demonstrating the synergism between vCyclin and vFLIP in BJAB cells, it implicates the presence of a cellular mechanism operative in BJAB, but defective in HeLa cells, that guards against overly active vCyclin/Cdk.

The cooperation between vCyclin and vFLIP as shown here allows NF-κB to be chronically activated in cells latently infected by KSHV. This facilitates cell proliferation, survival, immortalization, and rapid progression to malignancy during immunodeficiency. In contrast to KSHV, HTLV-1 lacks a vCyclin-like gene to mitigate the senescence response triggered by Tax. In HTLV-1-tranformed T cells where IKK/NF-κB is chronically activated by Tax, p27 expression is invariably down-regulated while p21 functionally inactivated by mis-localization to the cytoplasm[26,41], consistent with a loss of the senescence response. The loss/inactivation of the cellular senescence response in HTLV-1-transformed T cells is not, however, a virally encoded function. Rather, it is a result of cellular genetic or epigenetic changes selected during the process of *in vitro* HTLV-1 infection and T-cell transformation[26,41–43].

In conclusion, present studies of KSHV vCyclin and vFLIP and HTLV-1 Tax have revealed a mechanism by which NF-κB-induced G1 arrest/senescence response can be overridden by a G1 Cdk — vCyclin-Cdk6 — that resists p21/p27 inhibition and down-regulates p27 expression. They are consistent with the notion that the up-regulation of G1 Cdk activity, in addition to causing Rb inactivation and cell cycle entry, is obligatory for the development of chronic IKK/NF-κB activation. In this vein, we note that one of the most prominent features of ATL cells is the frequent loss of $p16^{INK4a}$ and $p15^{INK4b}$ [44–46], which likely increases cyclin D-Cdk activities and contributes to the dampening of the Tax/NF-κB-driven senescence response in the early stage of HTLV-1 leukemogenesis. Likewise, cyclin D1 and cyclin D3 are frequently over-expressed in multiple myeloma cells[25], which depend on chronically active NF-κB for survival[47]. The dependence of chronic NF-κB activation on constitutively up-regulated G1 Cdk as revealed by studying two human cancer viruses suggests that therapeutic strategies may be devised to drive relevant cancer cells into senescence or apoptosis by inhibiting Cdk or NF-κB.

Materials and Methods

Immunoblotting

Standard methods were used for immunoblotting. Briefly, cells were harvested and lysed. Protein concentration for each cell lysate was quantified using the Bio-Rad Protein Assay kit. Each sample loaded for immunoblotting typically contains 20–30 μg of cell proteins. HTLV-1 Tax mouse hybridoma antibody 4C5 was as described[22,26]. The rat hybridoma antibody against vFLIP was a kind gift of Dr. Mary Collins. Other antibodies used are from commercial sources as listed (supplemental Table S1).

Plasmids, lentiviral and adenoviral vectors

Lentiviral vectors for HTLV-1 Tax, KSHV vFLIP and vCyclin were constructed by insertion of the respective cDNA fragment into the BamHI and EcoRI restriction endonuclease sites of HR-CMV-SV-puro vector[28,41]. In another set of vectors, the puromycin resistant gene (puro) in HR-CMV-SV-Puro was replaced by the neomycin-resistance gene (neo). In all HR-CMV-based vectors, expression of the transduced gene is driven by a composite promoter comprising of HIV LTR and CMV immediate early enhancer/promoter. For construction of LV-vFLIP-puro and LV-2Flag-vCyc-puro, the

coding sequences of vFLIP and the dual Flag-tagged vCyclin (2Flag-vCyclin) were derived from murine retrovirus vectors for vFLIP[27] and vCyclin[40] respectively. For LV-vFLIP-Flag-puro, the cDNA encoding vFLIP tagged with a Flag epitope at its COOH-terminus was generated by PCR, and cloned into HR-CMV-SV-puro using the BamHI and EcoRI restriction endonuclease cleavage sites. Lentivirus vectors for HTLV-1 Tax, LV-Tax-neo and LV-Tax-puro, have been described previously[26,28,41].

To obtain the LV-2Flag-vCyclin-vFLIP vector, the cDNA corresponding to the spliced bicistronic transcript encoding vCyclin and vFLIP was generated by PCR from the lambda phage clone L54 that harbors the region of interest[48], and cloned into the pENTR/D-TOPO plasmid (Invitrogen). The PCR product encompasses the 3' portion of vCyclin coding sequence including the PstI site and the entire vFLIP coding sequence with an EcoRI site incorporated at the 3' end. The complete bicistronic 2Flag-vCyclin-vFLIP cDNA was then assembled by joining the 5' region of 2Flag-vCyclin in a BamHI and PstI fragment derived from LV-2Flag-vCyclin and the PstI and EcoRI fragment containing the remainder of the vCyclin sequence and the full vFLIP coding region. The cDNA of 2Flag-vCyclin-Tax was made by replacing the entire vFLIP ORF with that of Tax via NcoI and EcoRI restriction endonuclease sites. In lentivirus vectors containing the bicistronic constructs, the expression of vFLIP or Tax is driven by the IRES within the coding region of vCyclin. All cloned genes in the constructs were confirmed by DNA sequencing. The details of cloning procedures are available upon request. Recombinant lentiviruses were prepared in HEK293T cells using a standard three-plasmid transfection procedure as previously described[26].

Recombinant adenovirus vector Ad-Tax was grown and titrated as previously published[26].

Construction of stable cell lines

The ΔN-I-κBα/HeLa-G and 2Flag-vCyclin/HeLa-G cell lines, known as ΔN-I-κBαN4 and vCyc-G2 respectively, were constructed by transducing HeLa/18×21-EGFP (HeLa-G) cells[28] using LV-ΔN-I-κBα-neo and LV-2Flag-vCyc-puro lentivirus vectors. HeLa-G cells grown in DMEM containing 10% fetal bovine serum (FBS) were infected with the lentivirus vector of interest in the presence of 8 μg/ml of polybrene. Twenty four or forty-eight hours later, the medium was replaced with fresh DMEM containing 10% FBS and puromycin (1 μg/ml, *Sigma-Aldrich*) or G418 (800 μg/ml, Gibco). The transduced cells were selected for one week with change of medium every 3–4 days. Cell clones were then isolated in 96-well plates after limiting dilution, and confirmed for the expression of the gene of interest by immunoblotting.

shRNA knockdown

HeLa-G cell lines with stable knockdown of RelA, c-Rel, and RelB and p100 combination respectively had been previously described[22]. To knockdown vCyclin expression, a 24-nt sequence (5'-GTTCCTGCCAACGTCATTCCGCAG) in the coding region of vCyclin was targeted[49]. Double-stranded oligonucleotides containing the target sequence, a TCTCTTGAA loop, the complimentary sequence of the target, a TTTTT RNA polymerase III termination sequence, and CCGG (AgeI site) and AATT (EcoRI site) overhangs were generated and inserted into a lentiviral vector, pLKO.1, which had been digested by AgeI

and EcoRI. After confirmation by DNA sequencing, the plasmid was used to prepare the lentiviral vector for vCyclin knockdown. Cells harboring the shRNA construct were selected with puromycin. The efficacy of knockdown was assessed by immunoblotting. When necessary, single cell lines were isolated by limiting dilution.

Flow cytometry

Cells were harvested after trypsin treatment, washed twice with 2 ml of cold phosphate-buffered saline solution (PBS), resuspended in 0.5 ml of PBS, and fixed in 5 ml of 70% ethanol overnight at 4°C. Ethanol-fixed cells were then washed twice with 5 ml of cold PBS containing 1% bovine serum albumin and incubated for 30 min at 37°C in 1.0 ml of a solution containing propidium iodide (PI) (20 μg/ml) and RNase (1 mg/ml). The fixed cells were filtered through a 70-micron cell strainer (BD Falcon, Cat. 35–2350) to remove cell clumps. The cellular DNA content was determined by fluorescence-activated cell sorting (FACS) (EPICS XL-MCL flow cytometer; Beckman-Coulter). The percentages of cells in G0/G1, S, and G2/M phases of the cell cycle were computed using the ModFit LT software. Ordinate: cell numbers; abscissa: DNA content. The size distribution of cells was determined using the FlowJo software.

Senescence-associated β-galactosidase staining

HeLa-G cells were infected with LV-vFLIP-puro or LV-Tax-puro vectror for 24 or 48 hours, and then trypsinized and plated sparsely (approximately 5×10^4 per well) for single cells in a 6-well plate in DMEM containing 10% FBS and puromycin (1 μg/ml). After 3 to 4 days of puromycin selection, cells were fixed for 5 minutes and stained for the expression of the senescence-associated β-galactosidase (SA-β-gal) using a kit purchased from Sigma-Aldrich.

Supplementary Material

Refer to Web version on PubMed Central for supplementary material.

Acknowledgements

We thank Drs. Mary Collins, Johnan Kaleeba, and Emmy Verschuren for the vFLIP antibody, vFLIP cDNA, and vCyclin expression plasmid respectively. This work was supported by grants from the National Institutes of Health (R01CA140963 and RO1CA115884) and the USU intramural research program (RO73NV).

References

1. Ganem D. KSHV and the pathogenesis of Kaposi sarcoma: listening to human biology and medicine. J Clin Invest. 2010; 120(4):939–949. [PubMed: 20364091]
2. Dittmer D, Lagunoff M, Renne R, Staskus K, Haase A, Ganem D. A cluster of latently expressed genes in Kaposi's sarcoma-associated herpesvirus. J Virol. 1998; 72(10):8309–8315. [PubMed: 9733875]
3. Ganem D. KSHV infection and the pathogenesis of Kaposi's sarcoma. Annu Rev Pathol. 2006; 1:273–296. [PubMed: 18039116]
4. Low W, Harries M, Ye H, Du MQ, Boshoff C, Collins M. Internal ribosome entry site regulates translation of Kaposi's sarcoma-associated herpesvirus FLICE inhibitory protein. J Virol. 2001; 75(6):2938–2945. [PubMed: 11222719]

5. Fujimuro M, Hayward SD, Yokosawa H. Molecular piracy: manipulation of the ubiquitin system by Kaposi's sarcoma-associated herpesvirus. Rev Med Virol. 2007; 17(6):405–422. [PubMed: 17688306]
6. Hayward SD, Liu J, Fujimuro M. Notch and Wnt signaling: mimicry and manipulation by gamma herpesviruses. Sci STKE. 2006; (335) re4.
7. Liu J, Martin HJ, Liao G, Hayward SD. The Kaposi's sarcoma-associated herpesvirus LANA protein stabilizes and activates c-Myc. J Virol. 2007; 81(19):10451–10459. [PubMed: 17634226]
8. Verschuren EW, Jones N, Evan GI. The cell cycle and how it is steered by Kaposi's sarcoma-associated herpesvirus cyclin. J Gen Virol. 2004; 85(Pt 6):1347–1361. [PubMed: 15166416]
9. Rivas C, Thlick AE, Parravicini C, Moore PS, Chang Y. Kaposi's sarcoma-associated herpesvirus LANA2 is a B-cell-specific latent viral protein that inhibits p53. J Virol. 2001; 75(1):429–438. [PubMed: 11119611]
10. Yamaoka S, Courtois G, Bessia C, Whiteside ST, Weil R, Agou F, et al. Complementation cloning of NEMO, a component of the IkappaB kinase complex essential for NF-kappaB activation. Cell. 1998; (7):1231–1240. [PubMed: 9657155]
11. Sun SC, Ballard DW. Persistent activation of NF-kappaB by the tax transforming protein of HTLV-1: hijacking cellular IkappaB kinases. Oncogene. 1999; (49):6948–6958. [PubMed: 10602469]
12. Bagneris C, Ageichik AV, Cronin N, Wallace B, Collins M, Boshoff C, et al. Crystal structure of a vFlip-IKKgamma complex: insights into viral activation of the IKK signalosome. Mol Cell. 2008; 30(5):620–631. [PubMed: 18538660]
13. Field N, Low W, Daniels M, Howell S, Daviet L, Boshoff C, et al. KSHV vFLIP binds to IKK-gamma to activate IKK. J Cell Sci. 2003; 116(Pt 18):3721–3728. [PubMed: 12890756]
14. Chu ZL, Shin YA, Yang JM, Di Donato JA, Ballard DWLH. IKKgamma mediates the interaction of cellular IkappaB kinases with the tax transforming protein of human T cell leukemia virus type 1. J Biol Chem. 1999; (22):15297–15300. [PubMed: 10336413]
15. Jin DY, Giordano V, Kibler KV, Nakano H, Jeang KTLH. Role of adapter function in oncoprotein-mediated activation of NF-kappaB. Human T-cell leukemia virus type I Tax interacts directly with IkappaB kinase gamma. J Biol Chem. 1999; (25):17402–17405. [PubMed: 10364167]
16. Xiao G, Sun SC. Activation of IKKalpha and IKKbeta through their fusion with HTLV-I tax protein. Oncogene. 2000; (45):5198–5203. [PubMed: 11064457]
17. Grossman WJ, Kimata JT, Wong FH, Zutter M, Ley TJ, Ratner L. Development of leukemia in mice transgenic for the tax gene of human T-cell leukemia virus type I. Proc Natl Acad Sci U S A. 1995; 92:1057–1061. [PubMed: 7862633]
18. Matsumoto K, Shibata H, Fujisawa JI, Inoue H, Hakura A, Tsukahara T, et al. Human T-cell leukemia virus type 1 Tax protein transforms rat fibroblasts via two distinct pathways. J Virol. 1997; 71(6):4445–4451. [PubMed: 9151835]
19. Yamaoka S, Inoue H, Sakurai M, Sugiyama T, Hazama M, Yamada T, et al. Constitutive activation of NF-kappa B is essential for transformation of rat fibroblasts by the human T-cell leukemia virus type I Tax protein. EMBO J. 1996; 15(4):873–887. [PubMed: 8631308]
20. Hasegawa H, Sawa H, Lewis MJ, Orba Y, Sheehy N, Yamamoto Y, et al. Thymus-derived leukemia-lymphoma in mice transgenic for the Tax gene of human T-lymphotropic virus type I. Nat Med. 2006; 12(4):466–472. [PubMed: 16550188]
21. Guasparri I, Keller SA, Cesarman E. KSHV vFLIP is essential for the survival of infected lymphoma cells. J Exp Med. 2004; 199(7):993–1003. [PubMed: 15067035]
22. Zhi H, Yang L, Kuo YL, Ho YK, Shih HM, Giam CZ. NF-kappaB Hyper-Activation by HTLV-1 Tax Induces Cellular Senescence, but Can Be Alleviated by the Viral Anti-Sense Protein HBZ. PLoS Pathog. 2011; 7(4):e1002025. [PubMed: 21552325]
23. Swanton C, Mann DJ, Fleckenstein B, Neipel F, Peters G, Jones N. Herpes viral cyclin/Cdk6 complexes evade inhibition by CDK inhibitor proteins. Nature. 1997; 390(6656):184–187. [PubMed: 9367157]
24. Mann DJ, Child ES, Swanton C, Laman H, Jones N. Modulation of p27(Kip1) levels by the cyclin encoded by Kaposi's sarcoma-associated herpesvirus. EMBO J. 1999; 18(3):654–663. [PubMed: 9927425]

25. Chapman MA, Lawrence MS, Keats JJ, Cibulskis K, Sougnez C, Schinzel AC, et al. Initial genome sequencing and analysis of multiple myeloma. Nature. 2011; 471(7339):467–472. [PubMed: 21430775]
26. Kuo YL, Giam CZ. Activation of the anaphase promoting complex by HTLV-1 tax leads to senescence. EMBO J. 2006; 25(8):1741–1752. [PubMed: 16601696]
27. Grossmann C, Podgrabinska S, Skobe M, Ganem D. Activation of NF-kappaB by the latent vFLIP gene of Kaposi's sarcoma-associated herpesvirus is required for the spindle shape of virus-infected endothelial cells and contributes to their proinflammatory phenotype. J Virol. 2006; 80(14):7179–7185. [PubMed: 16809323]
28. Zhang L, Liu M, Merling R, Giam CZ. Versatile reporter systems show that transactivation by human T-cell leukemia virus type 1 Tax occurs independently of chromatin remodeling factor BRG1. J Virol. 2006; 80(15):7459–7468. [PubMed: 16840326]
29. Matta H, Chaudhary PM. Activation of alternative NF-kappa B pathway by human herpes virus 8-encoded Fas-associated death domain-like IL-1 beta-converting enzyme inhibitory protein (vFLIP). Proc Natl Acad Sci U S A. 2004; 101(25):9399–9404. [PubMed: 15190178]
30. Shimizu A, Baratchian M, Takeuchi Y, Escors D, Macdonald D, Barrett T, et al. Kaposi's Sarcoma-Associated Herpesvirus vFLIP and Human T Cell Lymphotropic Virus Type 1 Tax Oncogenic Proteins Activate I{kappa}B Kinase Subunit {gamma} by Different Mechanisms Independent of the Physiological Cytokine-Induced Pathways. J Virol. 2011; 85(14):7444–7448. [PubMed: 21593170]
31. Yang L, Kotomura N, Ho YK, Zhi H, Bixler S, Schell MJ, et al. Complex cell cycle abnormalities caused by human T-lymphotropic virus type 1 Tax. J Virol. 2011; 85(6):3001–3009. [PubMed: 21209109]
32. Bieleski L, Talbot SJ. Kaposi's sarcoma-associated herpesvirus vCyclin open reading frame contains an internal ribosome entry site. J Virol. 2001; 75(4):1864–1869. [PubMed: 11160685]
33. Grundhoff A, Ganem D. Mechanisms governing expression of the v-FLIP gene of Kaposi's sarcoma-associated herpesvirus. J Virol. 2001; 75(4):1857–1863. [PubMed: 11160684]
34. Lee JS, Li Q, Lee JY, Lee SH, Jeong JH, Lee HR, et al. FLIP-mediated autophagy regulation in cell death control. Nat Cell Biol. 2009; 11(11):1355–1362. [PubMed: 19838173]
35. Leidal AM, Cyr DP, Hill RJ, Lee PW, McCormick C. Subversion of autophagy by Kaposi's sarcoma-associated herpesvirus impairs oncogene-induced senescence. Cell Host Microbe. 2012; 11(2):167–180. [PubMed: 22341465]
36. Koopal S, Furuhjelm JH, Jarviluoma A, Jaamaa S, Pyakurel P, Pussinen C, et al. Viral oncogene-induced DNA damage response is activated in Kaposi sarcoma tumorigenesis. PLoS Pathog. 2007; 3(9):1348–1360. [PubMed: 17907806]
37. Farrell PJ, Allan GJ, Shanahan F, Vousden KH, Crook T. p53 is frequently mutated in Burkitt's lymphoma cell lines. EMBO J. 1991; 10(10):2879–2887. [PubMed: 1915267]
38. Ojala PM, Tiainen M, Salven P, Veikkola T, Castanos-Velez E, Sarid R, et al. Kaposi's sarcoma-associated herpesvirus-encoded v-cyclin triggers apoptosis in cells with high levels of cyclin-dependent kinase 6. Cancer Res. 1999; 59(19):4984–4989. [PubMed: 10519412]
39. Jarviluoma A, Koopal S, Rasanen S, Makela TP, Ojala PM. KSHV viral cyclin binds to p27KIP1 in primary effusion lymphomas. Blood. 2004; 104(10):3349–3354. [PubMed: 15271792]
40. Verschuren EW, Klefstrom J, Evan GI, Jones N. The oncogenic potential of Kaposi's sarcoma-associated herpesvirus cyclin is exposed by p53 loss in vitro and in vivo. Cancer Cell. 2002; 2(3): 229–241. [PubMed: 12242155]
41. Liu M, Yang L, Zhang L, Liu B, Merling R, Xia Z, et al. Human T-cell leukemia virus type 1 infection leads to arrest in the G1 phase of the cell cycle. J Virol. 2008; 82(17):8442–8455. [PubMed: 18596104]
42. Cereseto A, Diella F, Mulloy JC, Cara A, Michieli P, Grassmann R, et al. P53 functional impairment and high p21waf1/cip1 expression in human t-cell lymphotropic/leukemia virus type i-transformed t cells. Blood. 1996; 88(5):1551–1560. [PubMed: 8781409]
43. Cereseto A, Washington PR, Rivadeneira E, Franchini G. Limiting amounts of p27Kip1 correlates with constitutive activation of cyclin E-CDK2 complex in HTLV-I-transformed T-cells. Oncogene. 1999; 18(15):2441–2450. [PubMed: 10229195]

44. Yamada Y, Hatta Y, Murata K, Sugawara K, Ikeda S, Mine M, et al. Deletions of p15 and/or p16 genes as a poor-prognosis factor in adult T-cell leukemia. J Clin Oncol. 1997; 15(5):1778–1785. [PubMed: 9164185]

45. Hatta Y, Koeffler HP. Role of tumor suppressor genes in the development of adult T cell leukemia/lymphoma (ATLL). J Virol. 2002; 16(6):1069–1085.

46. Oshiro A, Tagawa H, Ohshima K, Karube K, Uike N, Tashiro Y, et al. Identification of subtype-specific genomic alterations in aggressive adult T-cell leukemia/lymphoma. Blood. 2006; 107(11): 4500–4507. [PubMed: 16484591]

47. Mitsiades N, Mitsiades CS, Poulaki V, Chauhan D, Richardson PG, Hideshima T, et al. Biologic sequelae of nuclear factor-kappaB blockade in multiple myeloma: therapeutic applications. Blood. 2002; 99(11):4079–4086. [PubMed: 12010810]

48. Russo JJ, Bohenzky RA, Chien MC, Chen J, Yan M, Maddalena D, et al. Nucleotide sequence of the Kaposi sarcoma-associated herpesvirus (HHV8). Proc Natl Acad Sci U S A. 1996; 93(25): 14862–14867. [PubMed: 8962146]

49. Godfrey A, Anderson J, Papanastasiou A, Takeuchi Y, Boshoff C. Inhibiting primary effusion lymphoma by lentiviral vectors encoding short hairpin RNA. Blood. 2005; 105(6):2510–2518. [PubMed: 15572586]

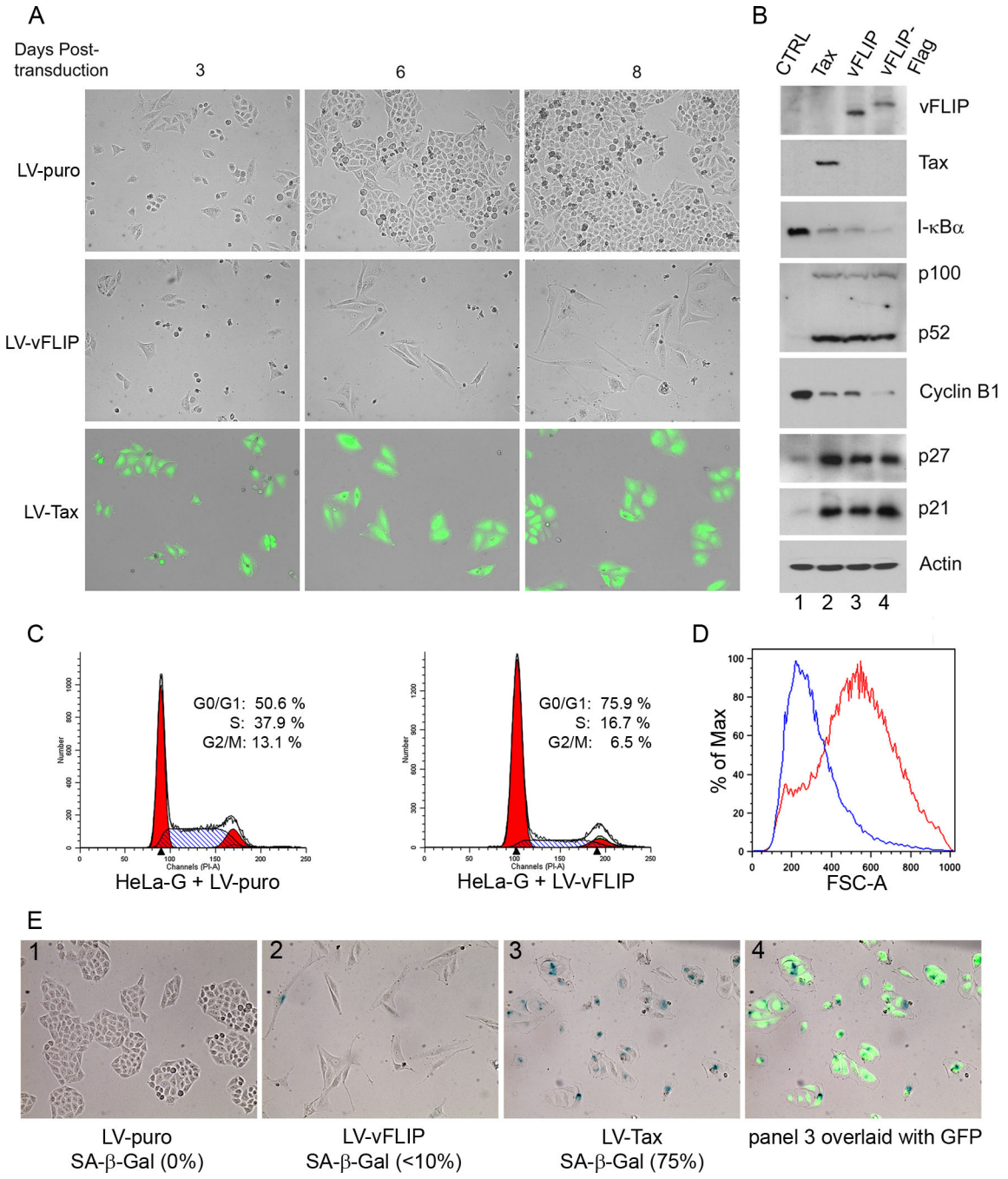

Figure 1. KSHV vFLIP induces G1 cell cycle arrest in HeLa cells

(A) HeLa-18×21-EGFP (HeLa-G) cells were transduced by LV-puro, LV-vFLIP-puro (LV-vFLIP) or LV-Tax-puro (LV-Tax) lentiviral vector respectively. Forty-eight hours after transduction, cells were seeded sparsely on 6-well plates in fresh medium containing 1 μg/ml puromycin. GFP expression in HeLa-G cells is under the control of 18 copies of a 21-bp Tax-responsive enhancer element that drives abundant GFP expression when Tax is expressed. The transduced cells were monitored microscopically. Photographs were taken at day 3, 6 and 8 after transduction. **(B)** Cells transduced with the control LV-puro vector

(CTRL) and the indicated lentiviral vectors for Tax, vFLIP, and Flag-epitope-tagged vFLIP (vFLIP-Flag) were selected in puromycin for 4 days, and then harvested for immunoblot analysis using antibodies against the proteins indicated on the right of each panel. The relative levels of I-κBα (1; 0.11; 0.08; 0.06), p52 (1; 22; 20; 18), cyclin B1 (1; 0.18; 0.18; 0.08), p27 (1, 8.7; 8.7; 9.3) and p21 (1; 6.6; 5.9; 8.0) in each lanes (lanes 1–4) were determined by densitometry, normalization against β-actin (Actin), and then fold changes computed by normalization again against the corresponding values of lane 1 control (CTRL). **(C)** Flow cytometry analysis of HeLa-G cells transduced with LV-puro (left panel) or LV-vFLIP-puro (LV-vFLIP, right panel). Transduced cells were selected with 1 μg/ml puromycin for 4 days. Puromycin-resistant cells were then harvested, fixed and stained with propidium iodide for flow cytometry. The percentage of cells in G1, S, and G2/M respectively was determined as in **Materials and Methods**. **(D)** The size distribution of cells was determined based on forward scatter and analyzed using the FlowJo software. Blue and red traces represent LV-puro- and LV-vFLIP-transduced cells respectively. **(E)** Senescence-associated β-gal staining of LV-puro, LV-Tax-puro or LV-vFLIP-puro-transduced cells was carried out as described in **Materials and Methods**.

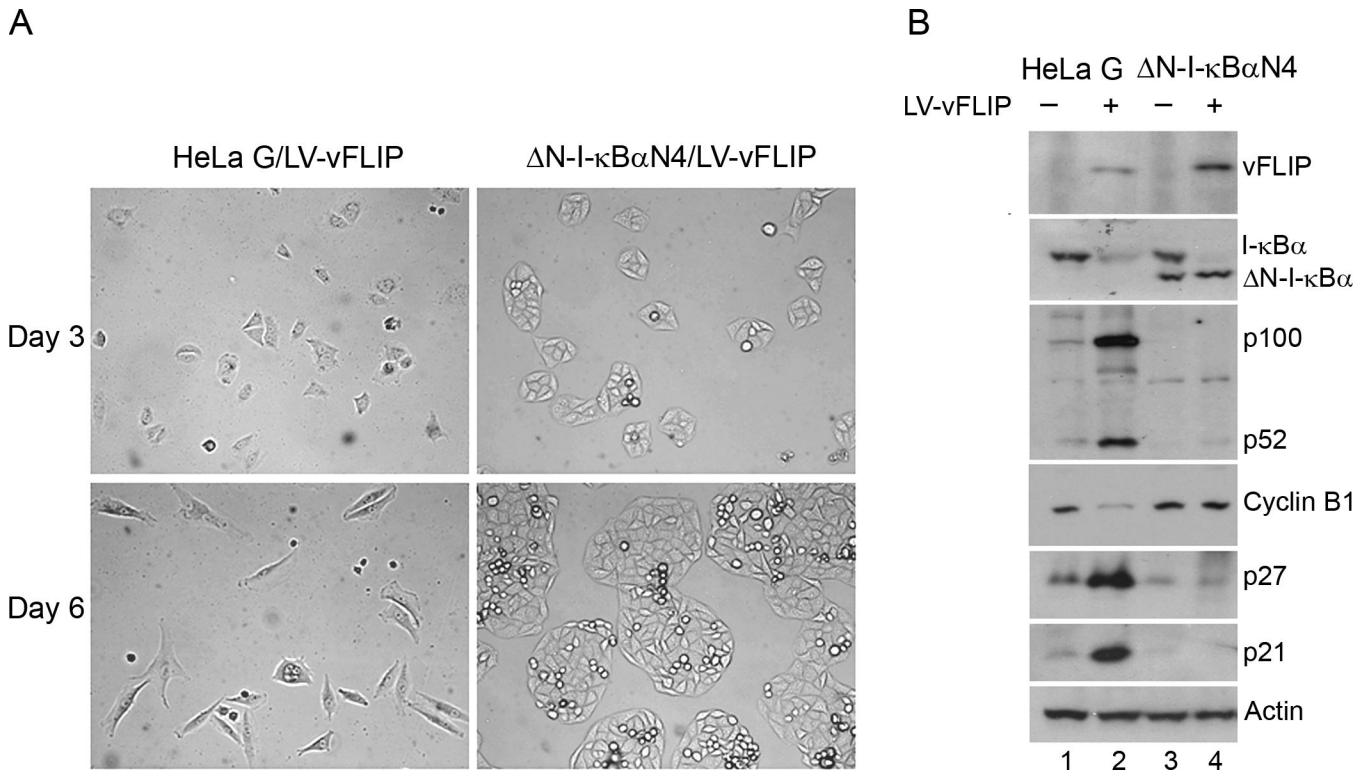

Figure 2. KSHV vFLIP-induced G1 arrest is NF-κB-dependent

(A) HeLa-G and its ΔN-I-κBα-expressing derivative, ΔN-I-κBαN4, were transduced with LV-vFLIP-puro and selected with puromycin as in Fig. 1. Cells were photographed at day 2 and 5 after puromycin selection. **(B)** Cells transduced with LV-puro or LV-vFLIP-puro were harvested four days after puromycin selection and analyzed by immunoblotting using the indicated antibodies.

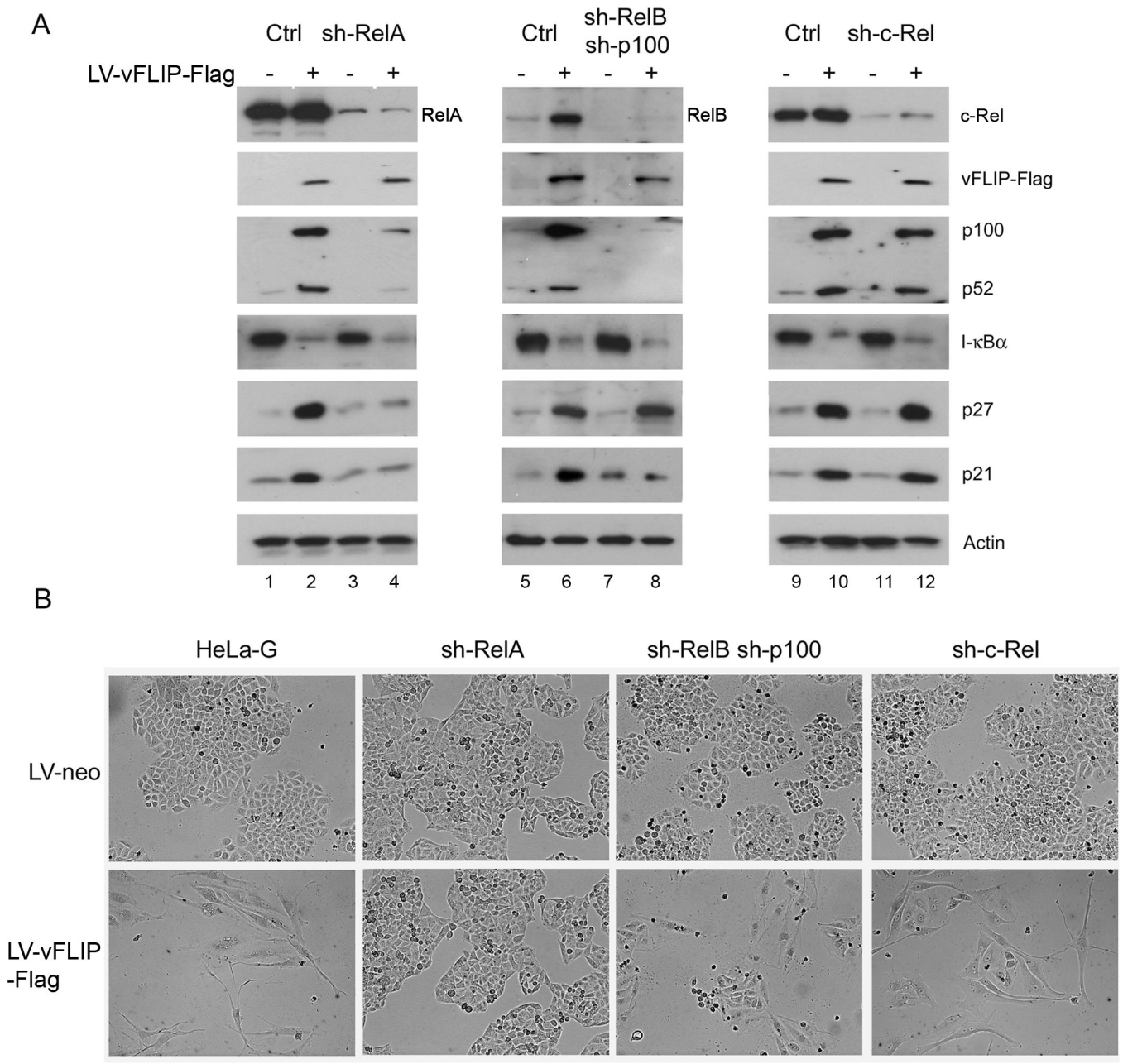

Figure 3. KSHV vFLIP-induced G1 arrest is driven by RelA

(A) HeLa-G cell line (Ctrl) and its progeny cell lines (sh-RelA, sh-RelB sh-p100, and sh-c-Rel) wherein RelA, RelB plus p100, and c-Rel respectively had been stably knocked down by small hairpin RNAs (shRNAs). In sh-RelB-p100 cell line, both RelB and p100 were knocked down to block the alternative NF-κB pathway. These cells were transduced with LV-neo or LV-vFLIP-Flag-neo, and selected with G418 (800μg/ml). The transduced cells were harvested 5 days after selection and analyzed by immunoblotting using antibodies indicated on the right. **(B)** Phase contrast photographs of LV-neo or LV-vFLIP-Flag-neo-transduced cells knocked down for various NF-κB family members on day 5 after G418 selection.

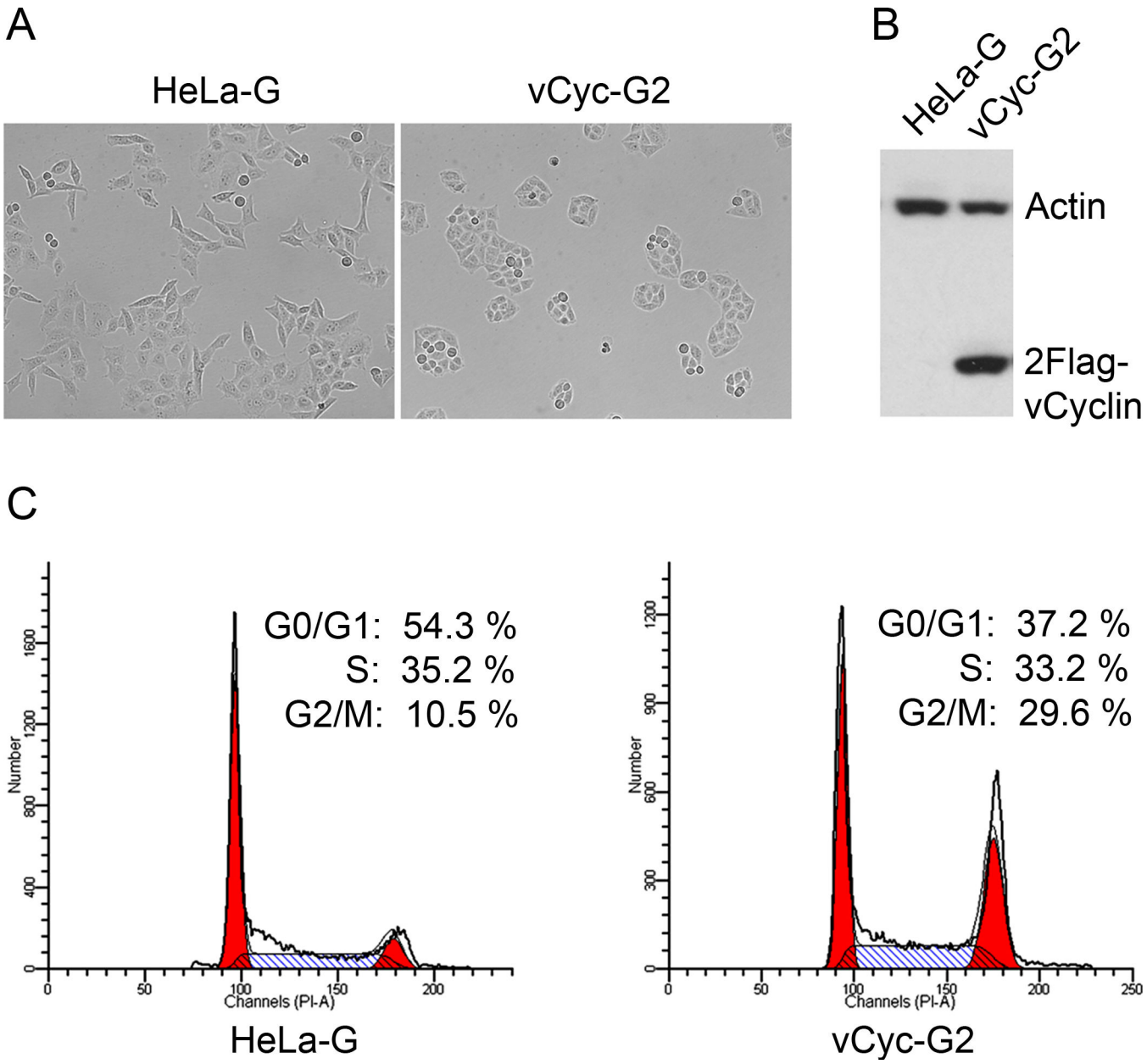

Figure 4. Characterizations of HeLa cells stably expressing KSHV vCyclin

(A) Phase contrast photographs of HeLa–G and its derivative, vCyc-G2, that expresses dual Flag-tagged- (2Flag-) vCyclin,. **(B)** Immunoblot analysis of HeLa–G and vCyc-G2 using a Flag-epitope antibody. **(C)** Flow cytometry histograms of HeLa-G and vCyc-G2. Exponentially growing HeLa-G and vCyc-G2 cells were subjected to flow cytometry as described in **Materials and Methods**. The percentage of cells in G1, S, and G2/M respectively was determined as in Fig. 1C.

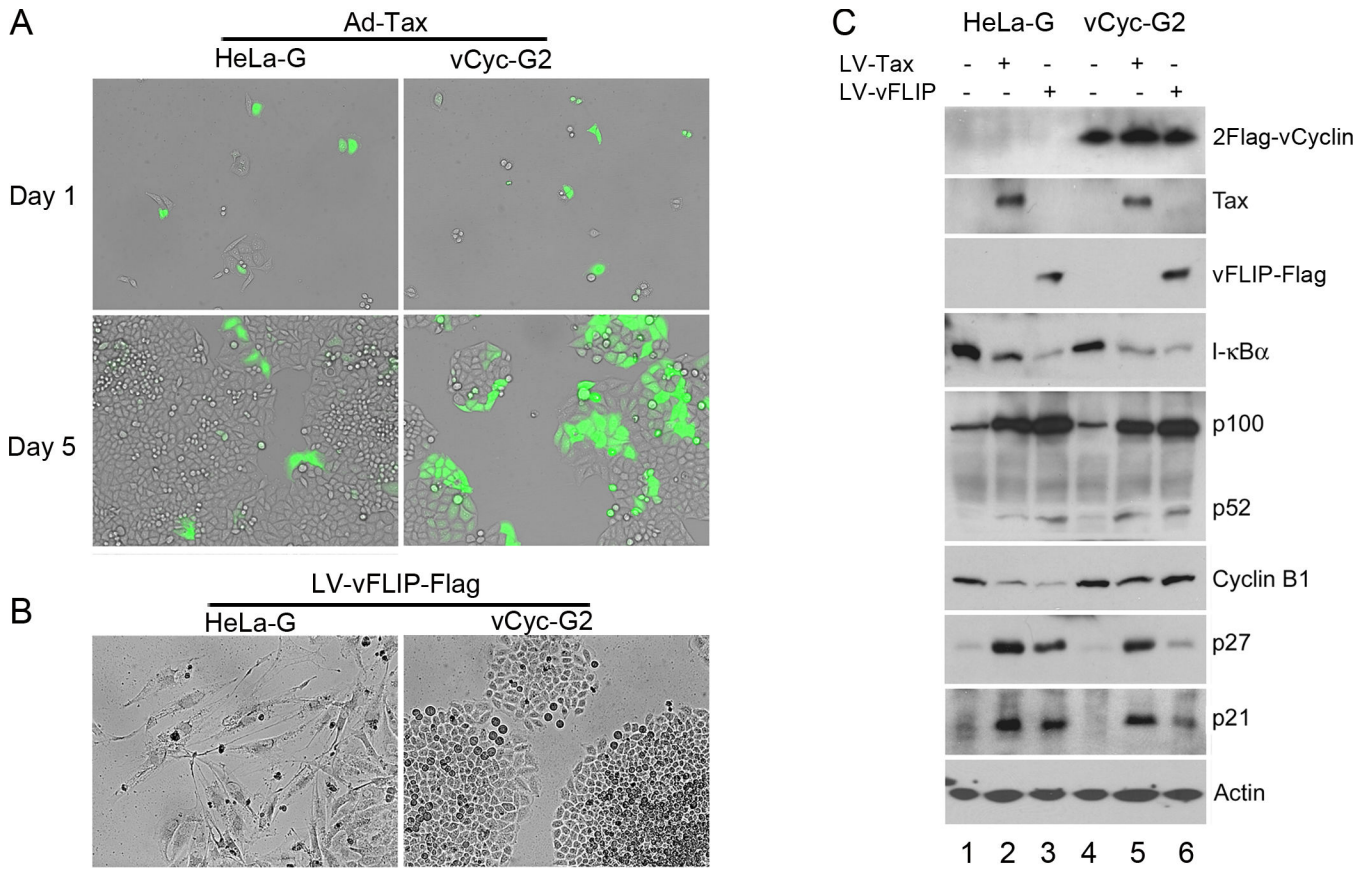

Figure 5. KSHV vCyclin prevents vFLIP- and HTLV-1 Tax-induced G1 arrest/senescence

(A) Phase contrast and fluorescent photographs of HeLa-G and vCyc-G2 cells transduced with Ad-Tax. Cells were transduced with Ad-Tax at an MOI of 1 to achieve approximately 30–50% transduction, and then plated sparsely as single cells. Photographs were taken at day 1 and day 5 after Ad-Tax transduction as indicated. GFP-positive cells were Ad-Tax-transduced. GFP-negative cells were un-transduced and served as internal controls. **(B)** Phase contrast photographs of HeLa-G and vCyc-G2 cells transduced with LV-vFLIP-Flag-neo and selected for 6 days with G418. **(C)** HeLa-G (lanes 1–3) and vCyc-G2 (lanes 4–6) were transduced with LV-neo (lanes 1 and 4), LV-Tax-Neo (Tax, lanes 2 and 5), and LV-vFLIP-Flag-neo (vFLIP, lanes 3 and 6) respectively as in Fig 1. After selection in G418-containing media for 4 days, the transduced cells were harvested and subjected to immunoblot analysis using the indicated antibodies. The relative levels of I-κBα (1; 0.29; 0.14; 1; 0.29; 0.16), p52 (1; 22; 20; 18), cyclin B1 (1; 0.29; 0.16; 1; 0.65; 0.88), p27 (1, 8.3; 6.3; 1; 5.8; 1.5) and p21 (1; 7.2; 6.8; 1; 6.1; 2.2) in each lanes (lanes 1–6) were determined as in Fig. 1B except that the final normalization was against the control lanes 1 (HeLa-G control) and 4 (HeLa-G/vCyc-G2) respectively.

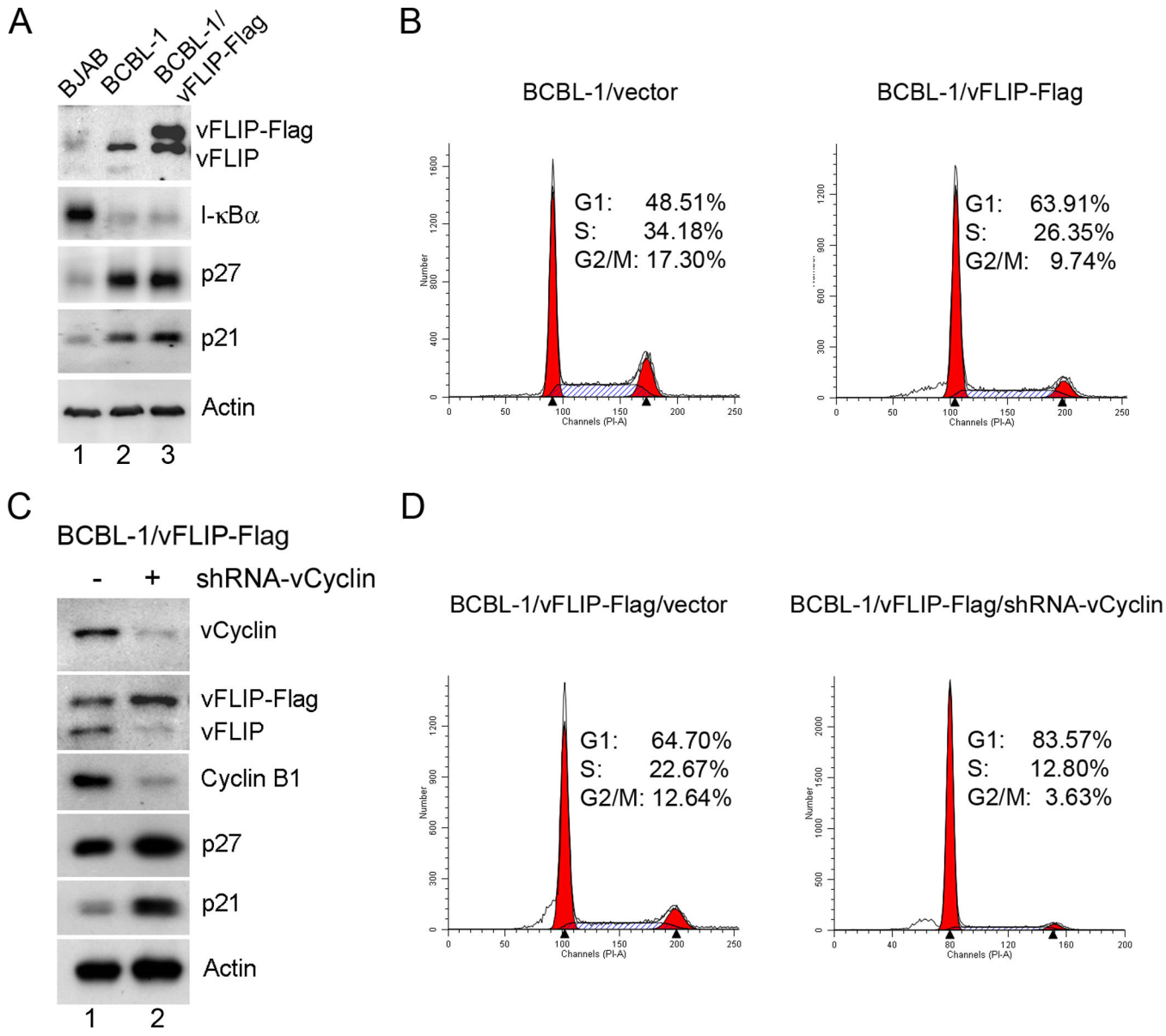

Figure 6. KSHV-transformed BCBL-1 cells that retain vFLIP, but are depleted for vCyclin arrest in G1 phase of the cell cycle

(A) BCBL-1 cells stably expressing exogenously added vFLIP-Flag were constructed by transduction with LV-vFLIP-Flag-neo, followed by G-418 selection. Immunoblotting was used to detect vFLIP-Flag and endogenous vFLIP expression, as well as the expression of I-κBα, p21, p27, and β-actin (Actin) (lane 3). Human BJAB B cells (lane 1) and LV-neo vector-transduced BCBL-1 cells (lane 2) were used as controls. (**B)** Flow cytometry histograms of LV-neo and LV-vFLIP-Flag-neo- transduced BCBL-1 cells. Exponentially and asynchronously growing cells were collected and subjected to flow cytometry analysis as in Fig. 1C. **(C)** The endogenous vCyclin and vFLIP in BCBL-1/vFLIP-Flag cells were knocked down by transduction of LV-shRNA-vCyclin-puro (lane 2). BCBL-1 cells transduced with an empty vector were used as control (lane 1). After 4 days of puromycin selection, cells were harvested for Immunoblotting using the indicated antibodies. **(D)** Flow

cytometry histograms of BCBL-1/vFLIP-Flag cells compared to their vCyclin-depleted counterparts (BCBL-1/vFLIP-Flag/shRNA-vCyclin).

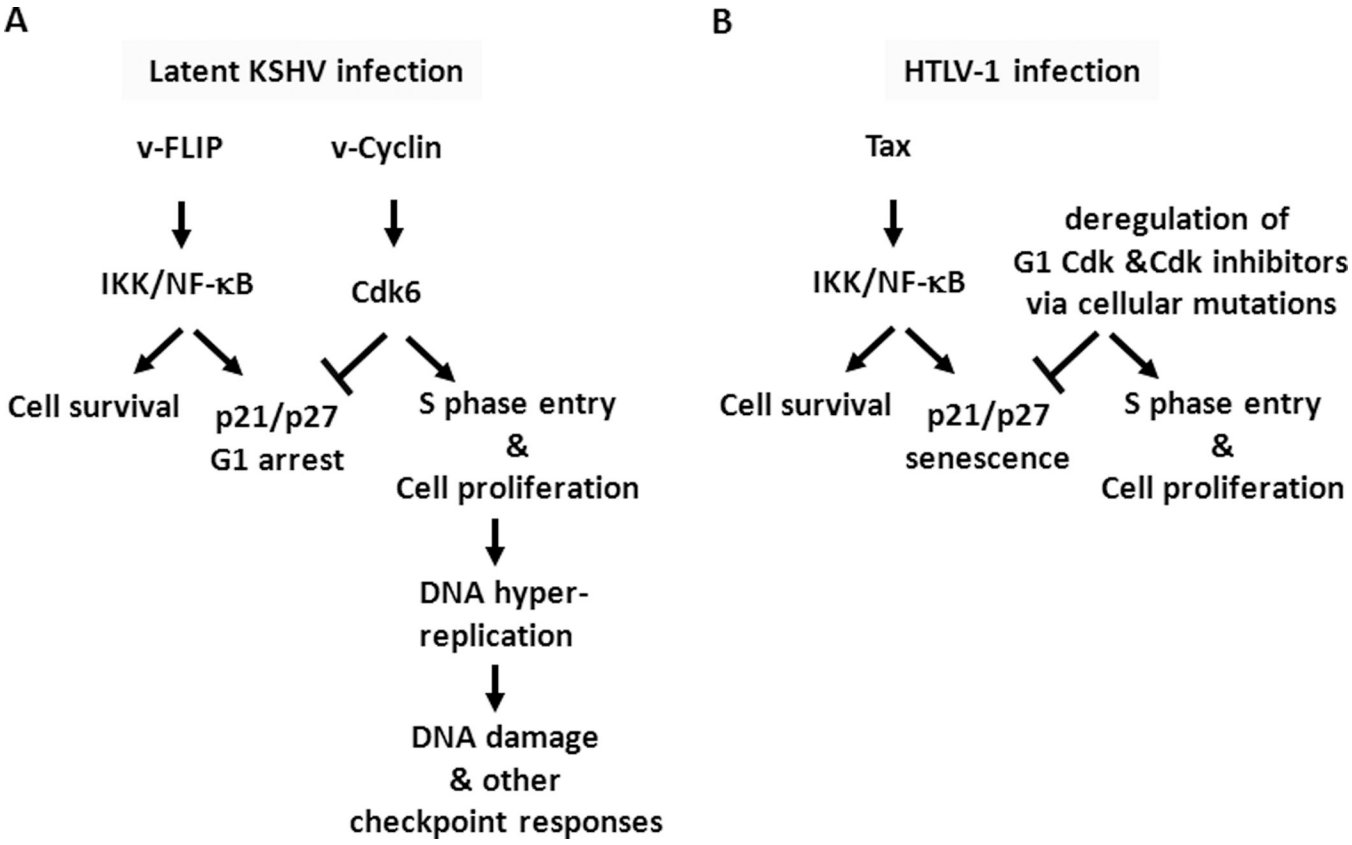

Figure 7. Roles of KSHV vFLIP and vCyclin, and HTLV-1 Tax in oncogenesis

(A) Synergistic actions of KSHV latency proteins vCyclin and vFLIP Cells latently infected by KSHV express vCyclin and vFLIP from a bicistronic latency mRNA transcript. NF-κB hyper-activation by vFLIP promotes cell survival, but triggers a host checkpoint response mediated by p21 and p27 that arrests cells in the G1 phase of the cell cycle. KSHV vCyclin binds and activates Cdk6 to promote S phase entry. The vCyclin/Cdk6 complex prevents the G1 arrest caused by vFLIP, thereby facilitating chronic NF-κB activation and cell survival. However, vCyclin expression also causes DNA hyper-replication and activates the DNA damage response or other checkpoints, which likely become inactivated by other viral factors or cellular oncogenic alterations. **(B) In HTLV-1 transformed cells, the senescence checkpoint response induced by Tax is inactivated by deregulation of G1 Cdks and Cdk inhibitors p21 and p27.** Hyper-activation of IKK/NF-kB by the HTLV-1 triggers cellular senescence checkpoint response, which is likely mitigated by somatic mutations that deregulate G1 Cdks and G1 Cdk inhibitors.